Exchange-hole dipole dispersion model for accurate energy ranking in molecular crystal structure prediction II: Non-planar molecules

Sarah R. Whittleton,[†] A. Otero-de-la-Roza,[‡] and Erin R. Johnson[*][,†]

Department of Chemistry, Dalhousie University, 6274 Coburg Road, Halifax, Nova Scotia, Canada B3H 4R2, and Department of Chemistry, University of British Columbia, Okanagan, 3247 University Way, Kelowna, British Columbia, Canada V1V 1V7.

E-mail: erin.johnson@dal.ca

Abstract

The crystal structure prediction (CSP) of a given compound from its molecular diagram is a fundamental challenge in computational chemistry with implications in relevant technological fields. A key component of CSP is the method to calculate the lattice energy of a crystal, which allows the ranking of candidate structures. This work is the second part of our investigation to assess the potential of the exchange-hole dipole moment dispersion (XDM) model for crystal structure prediction. In this article, we study the relatively large, non-planar, mostly flexible molecules in the first five blind tests held by the Cambridge Crystallographic Data Centre. Four of the seven experimental structures are predicted as the energy minimum, and thermal effects are demonstrated to have a large impact on the ranking of at least one other. As in the first part of this series, delocalization error affects the results for a single crystal (compound X), in this case by detrimentally overstabilizing the π-conjugated conformation of the monomer. Overall, B86bPBE-XDM correctly predicts 16 of the 21 compounds in the five blind tests, a result similar to the one obtained using the best CSP method available

to date (dispersion-corrected PW91 by Neumann et al.). Perhaps more importantly, the systems for which B86bPBE-XDM fails to predict the experimental structure as the energy minimum are mostly the same as with Neumann's method, which suggests that similar difficulties (absence of vibrational free energy corrections, delocalization error,...) are not limited to B86bPBE-XDM, but affect GGA-based DFT-methods in general. Our work confirms B86bPBE-XDM as an excellent option for crystal energy ranking in CSP, and offers a guide to identify crystals (organic salts, conjugated flexible systems) where difficulties may appear.

1 Introduction

First-principles molecular crystal-structure prediction (CSP) represents a grand challenge in the field of theoretical and computational chemistry. A reliable and efficient CSP method would be of enormous value in various scientific and technological fields, aiding in the design of new pharmaceuticals, organic electronics, and energetic materials, the properties of which are all strongly affected by crystal polymorphism.[1–10] The three principal facets of CSP are: generation of candidate structures, preliminary refinement and energy ranking to identify a short list of likely candidates, and accurate calculation of the lattice free energies to iden-

---

*To whom correspondence should be addressed
†Dalhousie University
‡University of British Columbia

tify the most stable crystal structure. Each of these aspects of CSP is the subject of active method development.

CSP strategies are routinely assessed through blind-test competitions conducted by the Cambridge Crystallographic Data Centre (CCDC),[11–16] in which computational methods are applied to compounds with experimentally-measured, but as-yet unpublished, crystal structures. Each research group participating in the blind test submits their top three candidate structures and these predictions are compared to the experimental structure to determine whether there is a match. Six CSP blind tests have been held to date. In the most recent of these,[16] dispersion-corrected density-functional theory (DFT) methods[17,18] were shown to be quite promising for the final energy-ranking step of a CSP protocol, albeit computationally expensive compared to earlier methods. Additionally, system-specific potentials fit to dispersion-corrected DFT results have performed extremely well in all 6 blind tests[16,19–22] and in pharmaceutical polymorph screening.[23]

An additional complication in first-principles CSP is that the crystal structure with the lowest electronic energy is not necessarily the experimentally observed one. In a recent force-field-based study,[24] it has been shown that the neglect of thermal and zero-point contributions to the lattice free energy alters the identity of the predicted thermodynamically stable structure for 9% of the compounds considered. In addition, it is known that different polymorphs of the same compound may crystallize under varying experimental conditions (e.g. from different solvents), which indicates that kinetic effects also play a role whose importance is at present unknown. Nevertheless, the success of DFT-based methods in recent blind tests[14–16] suggests that DFT approaches are able to determine, if not the experimentally observed structure, at least the crystal energy landscape of a given compound[25] with some degree of reliability.

In our own previous work,[26] the B86bPBE density functional[27,28] with the exchange-hole dipole moment (XDM) dispersion cor-

rection[29–31] was applied to a subset of 14 compounds considered in the first five CSP blind tests. This subset consisted of 11 planar or near-planar molecules, along with a co-crystal of two planar molecules, a hydrate, and an organic salt. For each of these compounds, full B86bPBE-XDM relaxations were performed for the structures submitted to the blind test competitions (three per group) to identify the lowest-energy form. It was found that B86bPBE-XDM correctly predicted the experimental structure to be lowest in energy for 13 of the 14 crystals considered. The exception was the organic salt, where DFT methods are not expected to perform well due to delocalization error (also called charge-transfer error).[32–36] Also, quasi-harmonic modeling of the thermal free-energy correction was found to be necessary for one of the compounds in order to obtain the experimental structure as the thermodynamic ground state.[26]

In this work, we consider the remaining seven compounds from the first five blind tests (Brandenburg and Grimme have assembled a separate benchmark for the compounds in the sixth blind test[37]). These molecules represent somewhat more complex cases for CSP than in our previous work since, being non-planar, there is a broader range of potential packing arrangements. An additional complicating factor is that many of these molecules are conformationally flexible, so an accurate treatment of both the intermolecular and intramolecular contributions to the lattice energy is required. The ability of B86bPBE-XDM for energy ranking of the candidate structures is assessed and it is found to identify the experimental crystal structure as lowest in energy for four of the seven compounds considered. Thermal corrections are found to be of critical importance for one of the remaining compounds, and in another compound the error in the prediction can be traced back to the intramolecular energy of different molecular conformations. The analysis of the successes and failures of B86bPBE-XDM, whose performance is similar to the previous DFT-based approaches used on the same crystals, provides insight into the strengths and weaknesses of DFT for the purpose of calcu-

lating relative energies of molecular crystals in general, and for molecular crystal structure prediction in particular.

2 Computational Methods

The computational methods used in this work are consistent with our previous study of energy ranking in molecular crystal structure prediction.[26] The initial geometries of all experimental and candidate crystal structures were taken from the supplementary information of the second through fifth CSP blind tests[12–15] (the first blind test[11] consisted entirely of planar and near-planar molecules, which were considered in our previous work[26]). The crystal geometries, including both cell dimensions and atomic positions, were fully relaxed using the B86bPBE[27,28] density functional and the XDM dispersion correction,[29,30] with version 4.3.2 of the Quantum ESPRESSO program.[38] These plane-wave/pseudopotential (PW/PS) calculations used the Projector Augmented Wave (PAW) method[39] with an 80 Ry plane-wave cutoff, an 800 Ry density cutoff, and a $4{\times}4{\times}4$ Γ-centered **k**-point grid. It is important to note that no re-parametrization of the two XDM damping function parameters has been done in this work. The B86bPBE-XDM method is, in every aspect, the same as the one we used in other previous calculations for the solid state, such as our recent work on surface adsorption energies.[40–42]

As in our previous work, the initial calculations used the default convergence criteria for the geometry relaxations. Subsequent calculations using the tighter convergence criteria of 10^{-5} Ry for the energy and 10^{-4} Ry/bohr for the forces were then performed on the structures found to be less than 0.4 kcal/mol higher in energy than experiment in order to resolve the small energy differences between polymorphs. However, unlike our previous work, it was not feasible to perform quasi-harmonic calculations to obtain thermal free-energy corrections for any near-degenerate structures due to the much larger unit-cell sizes. Instead, harmonic thermal free-energy corrections were ob-

tained using the Phonopy program[43] to calculate the phonon frequencies at the Γ point of the static equilibrium geometry.
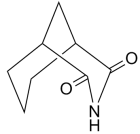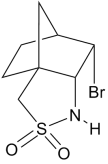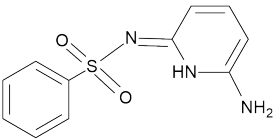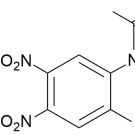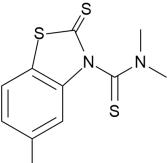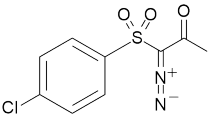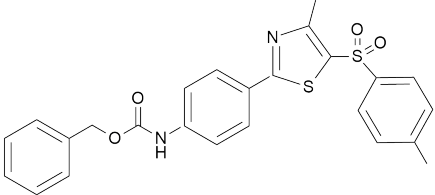
3 Results and Discussion

3.1 Energy ranking

The B86bPBE-XDM results for the seven compounds are summarised in Table 1. The notation was chosen to match that used in the blind tests, where the compounds are identified by roman numerals. The individual candidate structures are identified by the name of the participant group and the ranking (1, 2, or 3) within their submitted predictions. The relative energies for each candidate structure, relative to experiment, are shown in Figure 1. The upper panel of the figure shows results with both the dispersion-corrected and uncorrected base functional (both at the optimised B86bPBE-XDM geometries). The lower panel shows only the dispersion-corrected results for low-energy structures, close to or lower than the energy of the optimised experimental structure. B86bPBE-XDM was found to identify the experimental structure as lowest in energy for 4 of the 7 compounds. The exceptions are compounds V, X, and XX, for which 2, 1, and 3 unique candidate structure(s), respectively, were predicted to be more stable than the experimental form. Uncorrected B86bPBE predicts the correct experimental structure also in 4 out of 7 compounds. However, for compounds IV, XIV, and XX, very many candidates were predicted to lie lower in energy than the experimental form. In each of the cases where the base functional predicts the experimental structure not to be the energy minimum, it favours structures that have lower densities, as seen in our previous work.[26] This is to be expected since the dispersion energy will be minimized for more dense packings, so neglect of dispersion favours less dense structures.

Curiously, of the three systems in the second blind test (IV, V, and VI), B86bPBE-XDM succeeds for IV and VI but fails for V, whereas the reverse occurred for the methods

Table 1: Summary of XDM-corrected and base density-functional results. The number of the blind test (BT) in which the crystal structures were reported is indicated, along with the roman numeral which serves as the compound identifier. The ✓ symbol indicates that the experimental crystal structure was correctly predicted to be the lowest in energy. The ✗ symbol indicates that at least one other polymorph was predicted to be lower in energy than the experimental structure. The difference in energy between the most stable candidate and the experimental structure is also shown with and without XDM (ΔE_{XDM} and ΔE_{base}, both in kcal/mol per molecule). The latter was calculated at the B86bPBE-XDM equilibrium geometry.

Compound	Number	BT	XDM	Base	ΔE_{XDM}	ΔE_{base}
	IV	2	✓	✗	—	-1.16
	V	2	✗	✓	-0.54	—
	VI	2	✓	✓	—	—
	X	3	✗	✓	-0.44	—
	XIV	4	✓	✗	—	-1.60
	XVIII	5	✓	✗	—	-0.42
	XX	5	✗	✗	-1.13	-4.08

used by the participants. Van Eijck *et al.* and Price *et al.* gave the experimental structure of V as their first choice, whereas IV was correctly predicted only by Leusen-3 and Mooij-2, and none of the participants gave the experimental structure of VI as any of their top three candidates. The relatively poor performance of the CSP protocols at the time spurred a number of combined experimental and theoretical studies searching for experimental evidence of polymorphs for compounds IV and VI. Compound IV (3-azabicyclo[3.3.1]nonane-2,4-dione), whose experimental structure used in the blind test contains a catemer-like hydrogen-bonded network, was later crystallized in two additional forms, one of which is a plastic phase

Figure 1: Relative DFT-XDM energies for all submitted structures, ordered by blind test (blocks marked as 2, 3, 4, 5) in kcal/mol per molecule. The experimental structure is taken as the zero of energy in both plots. The top figure shows the dispersion-corrected (black) and uncorrected (purple) energies. The shaded region (± 1 kJ/mol around zero) represents the typical energy differences between isolable polymorphs.[24] The bottom plot shows the dispersion-corrected energies in a smaller region around zero. The red lines correspond to candidate structures that are not observed experimentally. The energies for the experimental structures are shown in green.
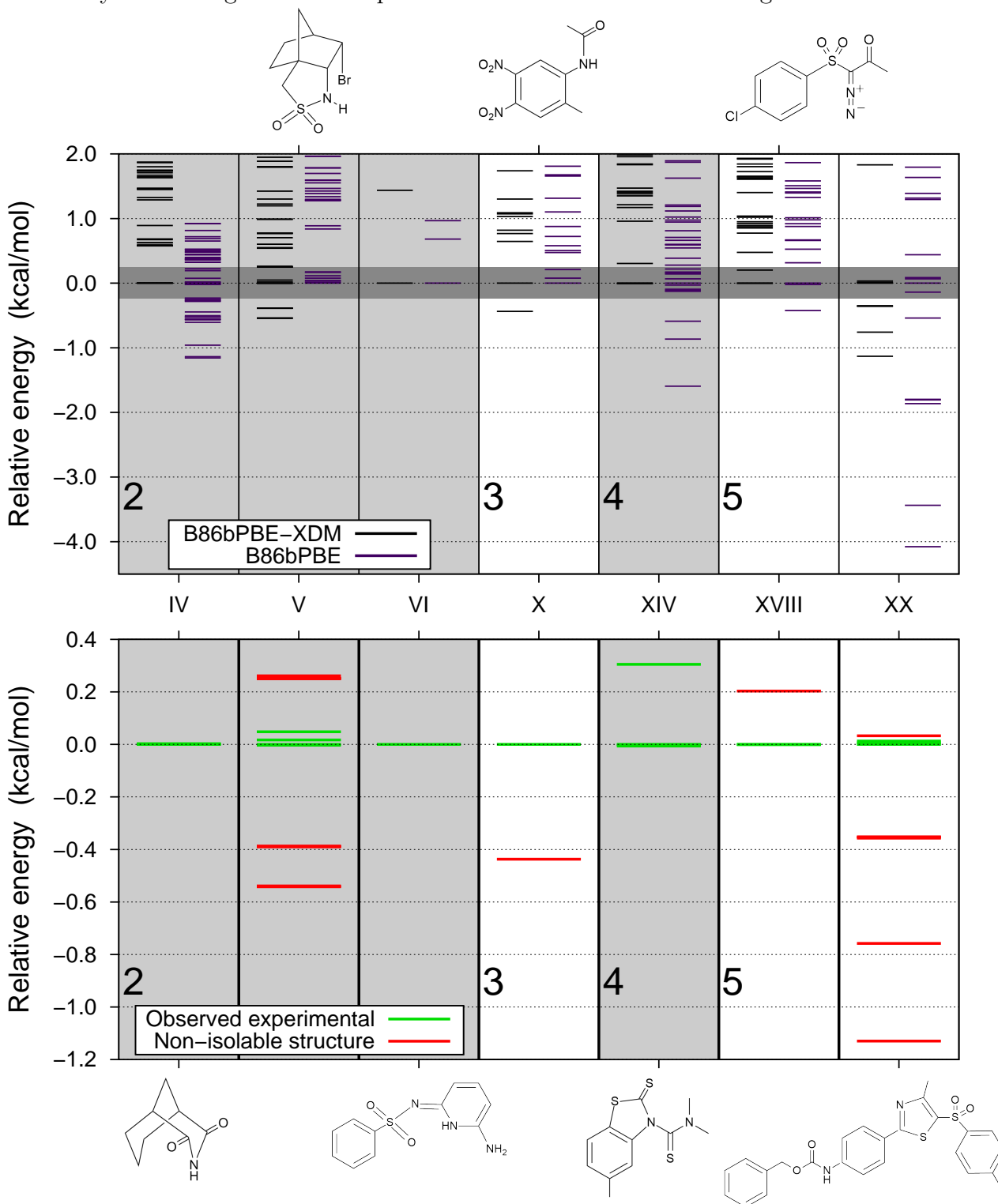
(see Ref. 44 and references therein). The weak nature of the imide hydrogen bond in this crystal caused most force field approaches to predict double-hydrogen-bonded dimers, rather than the correct catemer structure.[45] Two additional polymorphs of compound VI have also been found.[46,47] The fact that no other candidate structures appear in the ± 1 kJ/mol polymorphism energy range for compounds IV and VI in the present work may simply indicate that these structures were not among the top three candidates proposed by any of the blind test participants. For instance, using Neumann *et al.*'s force field, Chan *et al.* ranked forms II and III of compound VI as 20th and 140th, respectively.[48] As such, these forms would not have been selected as leading candidates, even though they were correctly ranked by the dispersion-corrected DFT method in the same work.

Neumann *et al.*[19] proposed a DFT-based approach for CSP, which they used in the fourth and fifth blind tests.[14,15] Although the force field used in their candidate structure generator, and for initial energy ranking, is based on system-specific empirical potentials ("tailor-made force fields"[49]) parameterized to reproduce dispersion-corrected[50] DFT results, the final ranking step uses a dispersion-corrected[19,50] PW91 functional.[51,52] Neumann *et al.*'s method was applied by Asmadi *et al.*[21] to the compounds in the first three blind tests. For the compounds in the second blind test, Asmadi *et al.* predicted the correct experimental structure for IV and VI, but failed for V, where the experimental structure was predicted to be 0.36 kcal/mol above the energy minimum (c.f. 0.54 kcal/mol for B86bPBE-XDM in Table 1). This remarkable agreement between two otherwise very dissimilar dispersion-corrected DFT methods is observed for the rest of the compounds, as discussed in Section 5, and indicates that general conclusions about the ability of dispersion-corrected DFT for CSP can be drawn from the present results.

Neumann's group also correctly predicted the experimental structure for both compounds XIV and XVIII, as does B86bPBE-XDM. However, for compound XIV, B86bPBE-XDM optimization of the Neumann-1 structure yields an energy that is 0.3 kcal/mol per molecule higher than that of the optimized experimental structure. Analysis of the structures using the overlap between calculated powder diffraction patterns (see Section 4) reveals that the two optimized structures are effectively identical (POW= 0.0166). The near, but not exact, degeneracy of these two structures is likely a consequence of the optimisation algorithm, which can converge to structures near, but not at, the energy minimum when the potential is quite flat.[26]

In the next few sections, we comment briefly on the compounds for which B86bPBE did not predict the experimental structure as the energy minimum. We propose a justification for these failures based on known shortcomings of our current approach, but the usual caveats apply. Particularly, kinetic effects during crystallization may result in an experimentally observed phase other than the thermodynamically stable one.

3.2 Compound V: Thermal corrections

Vibrational free-energy corrections can easily change the relative stability order of polymorphs pairs whose energies differ by less than 1–2 kJ/mol.[24,26] However, accurate determination of vibrational free-energy contributions is quite expensive computationally because it requires the evaluation of the phonon density of states in a collection of cell volumes around equilibrium. Such quasi-harmonic calculations are not practical using DFT for crystals with tens to hundreds of atoms in the unit cell, such as those featuring in the blind tests. Thus, recourse must be made to less sophisticated harmonic methods involving only numerical calculation of the phonon frequencies at the Γ point, which introduces errors into the final energetic ranking. The errors associated with calculating the ΔF_{vib} relative to experiment at the static equilibrium geometry are up to 0.3 kcal/mol relative to using the room temperature volume for the compound V structures with the smallest unit cells (Williams-I, and Mooij-2). These are

comparable to the errors from the use of only the Γ-point and the frozen-phonon method for the case of aspirin polymorphs.[53]

The phonon frequencies and the corresponding vibrational free energy corrections were computed for the observed experimental structure and all low-energy, non-isolable structures shown for compound V in the lower panel of Figure 1. The relative B86bPBE-XDM energies, with and without vibrational corrections are given in Table 2. In the absence of vibrational corrections, there are three unique candidate structures that are significantly lower in energy than experiment: Williams-1, Mooij-1 and Mooij-2. Several other participants also predicted the same structures as Mooij and co-workers for this compound, and they are also listed in Table 2. Compound V is a chiral molecule and the experimental structure corresponds to the enantiopure crystal.[54] The Williams-1 structure for this compound is a particularly interesting case since this structure has the Cc space group,[12] which is not possible for an enantiopure crystal (and as a result, data for this structure is not shown in Figure 1). Williams-1 is a racemic crystal containing both enantiomers.

Addition of the vibrational correction shifts all the other candidate structures higher in energy relative to experiment, with the single exception of the Mooij-3 structure. The vibrational free energy correction also brings the racemic Williams-1 structure to a higher energy than the experimental enantiopure crystal. While the calculated free-energies of Mooij-1 and Mooij-3 remain slightly more stable than experiment (by 0.05 and 0.18 kcal/mol per molecule, respectively) this is well below the expected error from the vibrational free energy correction or the B86bPBE-XDM lattice energies themselves. These observations reinforce the importance of vibrational free energy corrections, which are computationally very expensive to calculate properly, but can significantly re-order the energy ranking for near-degenerate structures.

3.3 Compound X: Conformational energy

Compounds VI, X, XIV, XVIII, and XX all share some degree of conformational flexibility, but it is only for compound X that the intramolecular geometries of the two lowest-energy forms differ significantly. As noted above, vanEijck-3 for compound X is predicted to be 0.44 kcal/mol per molecule lower in energy than experiment. The vibrational free energy correction increases this value to 0.71 kcal/mol per molecule.

The key difference between the vanEijck-3 and experimental structures is the intramolecular geometry. The monomers in these two crystals show different amounts of π-conjugation between the amide group and the phenyl ring (see Figure 2). The vanEijck-3 form has the amide nearly planar with respect to the phenyl ring, with a C–C–N–C dihedral angle of −8°. In this conformation, intramolecular conjugation is maximized, and the dominant intermolecular interaction is π-stacking (Figure 2, top left). In the experimental form, the amide group forms a C–C–N–C dihedral of −37° degrees with the phenyl ring, and conjugation between the amide group and the phenyl ring is partially disrupted. This amide rotation permits the formation of strong N–H···O intermolecular hydrogen bonds (Figure 2, lower left).

Thus, the relative energies of these two structures are controlled by a subtle interplay between intramolecular conjugation and intermolecular H-bonding. In order to correctly rank the energies of these two forms, both the intermolecular and intramolecular interactions must be modeled accurately. However, it is well known that density functionals of the generalised-gradient-approximation (GGA) type over-stabilise conjugated systems.[55,56] This will cause the energy penalty required to twist the amide group out of plane to be overestimated with the B86bPBE[27,28] GGA functional used in this work.

A potential energy surface (PES) for rotation about the C–C–N–C dihedral was computed using the Gaussian 09 program.[57] Molecular geometries were optimized for seven constrained

Table 2: Relative DFT-XDM energies for selected low-energy structures of compound V, in kcal/mol per molecule. The relative electronic energies (ΔE), the vibrational correction to the free energy (ΔF_{vib}), and the relative Helmholtz free energies at 298 K (ΔF) are shown. For the sets of degenerate structures, phonon calculations were performed on only one of them.

Structure	ΔE	ΔF_{vib}	ΔF	Other Degenerate Structures
Expt	0.00	0.00	0.00	Ammon-1, Price-1, Williams-2
Williams-1	-0.63	0.77	0.14	Non-chiral space group
Mooij-1	-0.54	0.49	-0.05	Leusen-1, Verwer-2
Mooij-2	-0.39	0.66	0.27	Motherwell-3, Price-2, Williams-3
Mooij-3	0.25	-0.43	-0.18	Ammon-3, Gavezzotti-3, Verwer-3
Dzyabchenko-2	0.26	0.55	0.81	–

Figure 2: Two interacting molecules extracted from the crystals of the Experimental (top left) and vanEijck-3 (bottom left) structures for compound X. Close NH–O contacts are highlighted in green. The potential energy curve for rotation about the C–C–N–C dihedral (right) is also shown, with this dihedral highlighted. The PES was computed with four XDM-corrected density functionals and with MP2. The zero of energy corresponds to the dihedral angle value in the vanEijck-3 structure, which was predicted to be lowest in energy with B86bPBE-XDM.
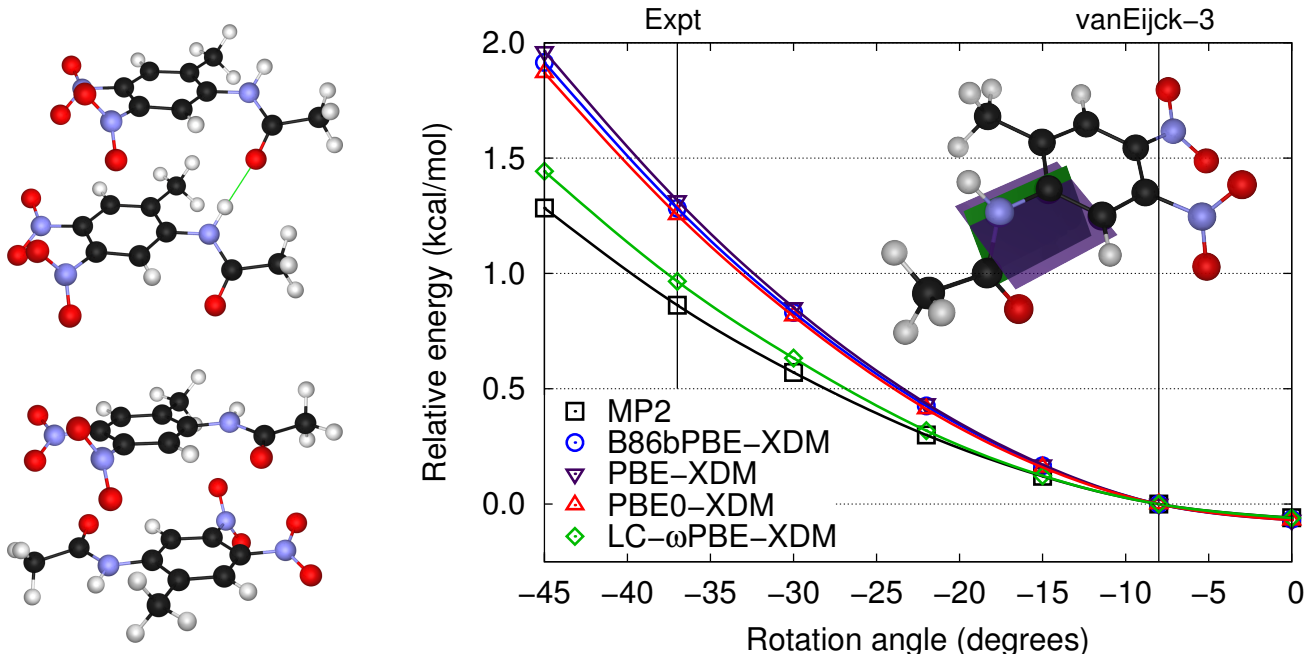
values of the dihedral between $-45°$ and $0°$ using PBE-XDM/pc-2-spd.[28,58–62] Subsequent single-point energy calculations were performed with selected methods using the larger aug-cc-pVTZ basis set: PBE-XDM,[28] B86bPBE-XDM,[27,28] PBE0-XDM,[63] LC-ωPBE-XDM[64,65] (psi4[66] was used for the B86bPBE functional, since it is not implemented in Gaussian). Single-point MP2/aug-cc-pVTZ calculations at the optimized geometries were also performed to provide an accurate reference curve.

The resulting PES is plotted in the right panel of Figure 2. Being both based on GGAs, the PBE-XDM and B86bPBE-XDM curves are essentially coincident. Figure 2 shows that, as more exact exchange is included in the functional, the barrier to rotation is reduced. LC-ωPBE-XDM is expected to be the most accurate of the four density functionals considered since it is the only one to include full long-range exact exchange. It is found to be in the best agreement with MP2 and

both give consistently lower energy penalties for rotation than B86bPBE-XDM, PBE-XDM, or PBE0-XDM. Using the MP2 value as the reference, B86bPBE-XDM under-stabilises the experimental conformation by 0.68 kcal/mol, which is higher than the lattice energy difference between vanEijck-3 and experiment (0.44 kcal/mol per molecule).

Table 3 shows that this effect is not limited to vanEijck-3 and the experimental structure, but it affects the other candidate structures as well. If the conformational energies of the monomers at their geometries in the crystal structure are calculated using MP2, instead of B86bPBE-XDM, the ranking of all candidate structures in a 3 kcal/mol energy range above experiment changes significantly. The relative energies also change, some by as much as 1.1 kcal/mol. Using MP2 for the intramolecular interactions gives the experimental structure as the most stable. These results shows that for flexible molecules, it is very important to have an accurate method for both the intermolecular and intramolecular energies. In this particular instance, GGA functionals are not sufficiently accurate for intramolecular energies due to their tendency to favour extended conjugation. However, a similar objection can be applied to the erroneous GGA description of intramolecular X-H bond stretching caused by the formation of a hydrogen bond,[67] which can be significant compared to the lattice energy differences typical in CSP.

The lattice energies relative to experiment corrected using LC-ωPBE-XDM conformational energies for each candidate structure in this work are shown in the Supporting Information (SI). Only the energy rankings in compounds X and XX (see below) are significantly affected. However, the conformational energy differences between B86bPBE-XDM and LC-ωPBE-XDM can be as large as 2.6 kcal/mol (for compound XVIII), which indicates that monomer deformation should be considered as a potential source of error when using dispersion-corrected GGA functionals.

3.4   Compound XX

B86bPBE-XDM fails to predict the experimental structure as the energy minimum in compound XX. Of the calculated structures, Price-2 (-1.13 kcal/mol), Neumann-2 (-0.76 kcal/mol), and the degenerate structures of Neumann-3, vanEijck-2, and vanEijck-3 (-0.35 kcal/mol), are all more stable than experiment. Interestingly, Neumann-1 is slightly higher in energy than the experimental structure (0.03 kcal/mol), according to B86bPBE-XDM. The experimental structure of compound XX was successfully predicted by Day's and by Price's group, both as their first candidate.

Compound XX appears to be a particularly challenging case for CSP using DFT. The experimental form was the 7th-ranked candidate in Neumann's work[15] and the 4th-ranked candidate with B86bPBE-XDM. This is not surprising as this is both the largest and most flexible of the compounds considered in the CSP blind tests and errors in the predicted lattice energies are expected to grow with system size and with the number of potential energy minima.[22] The difference in the conformational energies for the different monomers at their crystal geometries between B86bPBE-XDM and LC-ωPBE-XDM span an energy range of up to 1.67 kcal/mol. In addition, it is likely that thermal corrections are of importance in compound XX, but the unit cell for many of the candidate structures, including the experimental one, is too large to permit even the harmonic estimation of the vibrational free-energy correction with PW/PS DFT (220 atoms).

4   Equilibrium geometries

Table 4 compares the B86bPBE-XDM equilibrium geometries, as well as the geometries submitted by the blind test participants (for all cases identified as an experimental match) to the experimental crystal structures. "POW" indicates an adimensional similarity index based on the overlap between calculated powder diffraction patterns[68] evaluated using the critic2 program.[69] The other "RMSD$_{15}$" similarity index reported in the table is con-

Table 3: Re-ranking of a subset of the candidate structures for compound X induced by recalculating the monomer conformational energy with MP2/aug-cc-pVTZ. The columns are, in order: lattice energies of a subset of the candidate structures for compound X relative to experiment using B86bPBE-XDM (ΔE_{crys}) and the corresponding candidate ranking (Rank), the difference between conformational energies calculated with B86bPBE-XDM and MP2 (ΔE_{mon}), and the resulting lattice energy and ranking using the MP2 conformational energies. The recalculated ΔE_{crys} is the B86bPBE-XDM value plus ΔE_{mon}.

| | B86bPBE-XDM | | | B86bPBE-XDM+MP2 | |
Structure	ΔE_{crys}	Rank	ΔE_{mon}	ΔE_{crys}	Rank
Expt	0.00	2	0.00	0.00	1
Ammon-1	2.04	13	-0.50	1.54	10
Ammon-2	1.07	7	-0.48	0.59	4
Ammon-3	1.09	8	-0.19	0.90	7
Day-1	0.77	4	0.61	1.38	8
Day-2	1.03	6	0.36	0.68	6
Day-3	1.30	9	1.18	2.48	14
Dzyabchenko-1	2.11	14	0.80	2.91	16
Dzyabchenko-2	2.37	15	0.46	2.83	15
Dzyabchenko-3	0.65	3	-0.07	0.58	3
Erk-1	2.63	16	-0.17	2.45	13
Erk-2	2.01	11	-0.44	1.57	11
Erk-3	2.01	12	-0.44	1.57	12
vanEijck-1	1.74	10	-0.23	1.51	9
vanEijck-2	0.82	5	-0.18	0.64	5
vanEijck-3	-0.44	1	0.68	0.24	2

sistent with that used in the blind tests. It is evaluated by selecting molecular environments containing 15 molecules from each of the crystals to be compared, and then calculating the RMSD between the two environments in the situation of maximum overlap using the Mercury program.[70] For both similarity indices a value of zero indicates a perfect match. The POW index is more sensitive to changes in the intermolecular geometry while the RMSD_{15} is more sensitive to intramolecular distortions.

The results in Table 4 show that B86bPBE-XDM provides equilibrium geometries that are in very good agreement with the experimental crystal structures. It is important to note that the neglect of vibrational expansion in our DFT calculations (and in most methods presented in Table 4), causes an unavoidable disagreement with the experimental structure, estimated to be around 5–10% of the cell volume on average.[71] The B86bPBE-XDM values in Table 4 are consistent with the rest of

the blind test crystals examined in our previous work.[26] For the intramolecular geometries, as measured by the RMSD_{15}, B86bPBE-XDM consistently provides the best agreement with experiment, except for compound XIV, for which B86bPBE-XDM gives a slightly higher RMSD than Neumann-1. For the intermolecular packings, several other crystal geometries, particularly those from Neumann's group, are better matches to experiment than B86bPBE-XDM. However, it must be pointed out that the damping function in the dispersion correction used by Neumann et al. was fit using experimental low-temperature crystal structures, therefore including spurious vibrational effects in the electronic structure calculation.[19]

Table 4: Similarity indices comparing the DFT-XDM equilibrium structure (B86bPBE-XDM) and those submitted by the blind test participants to the corresponding experimental structures. The powder diffraction index (POW) computed using the critic2 program[69] and the RMSD index ($RMSD_{15}$ in Å) computing using the mercury program[70] are shown. For all cases, all 15 molecules in the environment used to calculate the RMSD match between the compared structures.

Number	Structure	POW	$RMSD_{15}$
IV	B86bPBE-XDM	0.1783	0.125
IV	Leusen-3	0.1070	0.227
IV	Mooij-2	0.0609	0.174
V	B86bPBE-XDM	0.0366	0.119
V	Ammon-1	0.0832	0.324
V	Price-1	0.0709	0.309
V	Williams-3	0.0984	0.264
VI	B86bPBE-XDM	0.0600	0.322
X	B86bPBE-XDM	0.0350	0.071
XIV	B86bPBE-XDM	0.0829	0.128
XIV	Neumann-1	0.0236	0.125
XIV	Price-1	0.0903	0.213
XIV	vanEijck-1	0.0306	0.146
XVIII	B86bPBE-XDM	0.0118	0.084
XVIII	Neumann-1	0.0379	0.122
XX	B86bPBE-XDM	0.0230	0.127
XX	Day-1	0.1042	0.429
XX	Price-1	0.0315	0.178

5 Comparison with an alternative CSP method

As mentioned in Section 3.1, Neumann and collaborators employed a combination of force-field and dispersion-corrected DFT calculations in the fourth and fifth blind tests,[14,15] with very good results compared to pure force-field approaches. In a study similar to this work, Asmadi et al.[21] retroactively applied Neumann's method to re-rank the candidate structures in the first three blind tests.[11–13] These results, combined with our present work, offer an excellent opportunity to identify patterns in the performance of dispersion-corrected DFT methods, since the dispersion correction (constant-coefficient D2-style) and the base functional (PW91) used by Neumann et al. are completely different from B86bPBE-XDM.[20–22]

Table 5: Comparison of the performance of B86bPBE-XDM and the PW91-D method of Neumann et al.[20–22] for crystal-structure prediction. For each compound in the first 5 CSP blind tests, the predicted rank of the experimental structure is given (1 is lowest in energy). For cases where the experimental structure was not ranked first, the energy difference, in kcal/mol per molecule, between it and the putative minimum-energy structure is tabulated.

| | Number | DFT-XDM | | PW91-D | |
		Rank	ΔE	Rank	ΔE
BT1	I	1	–	1	–
	II	3	0.25	2	0.01
	III	1	–	1	–
	VII	1	–	1	–
BT2	IV	1	–	1	–
	V	3	0.54	4	0.37
	VI	1	–	1	–
BT3	VIII	1	–	1	–
	IX	1	–	a	a
	X	2	0.44	1	–
	XI	1	–	1	–
BT4	XII	1	–	1	–
	XIII	1	–	1	–
	XIV	1	–	1	–
	XV	1	–	1	–
BT5	XVI	1	–	1	–
	XVII	1	–	1	–
	XVIII	1	–	1	–
	XIX	7	1.11	3	1.61
	XX	4	1.13	7	0.45
	XXI	2^b	0.15	81^b	2.12
		1^c	–	174^c	2.70

^{a}Calculations were not performed because the empirical dispersion correction was not parameterized for iodine.[21] ^{b}The same H arrangement as the proposed experimental structure. ^{c}An alternative H arrangement suggested by Price[15] and confirmed as lower in energy by DFT-XDM.[26]

The predicted energy rankings of the

experimentally-observed form of all 21 compounds included in the first 5 blind tests are reported for both B86bPBE-XDM and Neumann's method (termed PW91-D) in Table 5. B86bPBE-XDM (without vibrational free-energy corrections) correctly predicts the experimental structure as the lowest in energy for 16/21 compounds, while the success rate for the PW91-D method of Neumann *et al.* is 15/20 compounds.

Interestingly, four of the cases where the incorrect ranking is predicted are the same in both methods (compounds II, V, XIX, and XX). This may be due to neglect of vibrational or kinetic effects. Vibrational free-energy corrections have been shown to improve the B86bPBE-XDM rankings for compounds II and V, and this is potentially the case for compound XX as well. Thus, vibrational effects upset the identity of the lowest-energy structure for 10–14% of the crystals considered, which is consistent with the 1/9 ratio suggested by Nyman and Day[24] for a much larger data set. For compound XIX, the organic salt, the origin of the poor energy ranking can be traced to delocalization error[32–36] inherent in the base density-functional approximation, as discussed in our previous study.[26] The base density functionals used in the two methods (B86bPBE[27,28] and PW91[51,52]) are both GGAs and will thus be affected by delocalization error to a similar extent.

For compound X, PW91-D obtains the correct ranking, while B86bPBE-XDM does not. However, Neumann's group did predict vanEijck-3 (the B86bPBE-XDM minimum) as their 2nd-ranked structure, only 0.19 kcal/mol per molecule higher in energy than the experimental form. This may seem at odds with the discussion in Section 3.3, but it is important to note that PW91 has a tendency to overstabilize hydrogen bonds compared to other functionals.[72] Since the experimental structure has a hydrogen bond, but vanEijck-3 does not, the overstabilization of hydrogen bonds by PW91 cancels with the overstabilization of the almost-planar π-conjugated system.

For compound XXI, B86bPBE-XDM recovers the correct ranking, while the experimental structure is either the 81st or 174th ranked structure with PW91-D, depending on the hydrogen-atom arrangement.[15] This highlights the potential pitfalls of using empirical dispersion corrections with fixed coefficients. Compound XXI (gallic acid monohydrate) involves hydrogen bonds between the carboxylic acid groups and the intercalated water molecules. It would appear that such hydrates are problematic for PW91-D. Also a "difficulty in treating water with a point charge model and isotropic vdW parameters" in the tailor-made force field used for pre-screening was previously noted.[22]

Other DFT-based methods for energy ranking in CSP have been used in the recent sixth blind test,[16] most notably the TPSS-D3 method by Grimme et al. and PBE-MBD by Tkatchenko et al. It is difficult to compare the performance of B86bPBE-XDM to these methods, since the systems studied in the sixth blind test are different than in this and our previous article. Judging by the results presented in the sixth blind test, and the subsequent article by Brandenburg and Grimme,[37] both methods show excellent performance. (The poor results of TPSS-D3 in the sixth blind test can be attributed to the computationally cheaper HF-3c method used for the prescreening[37]). However, Table 6 in Ref. 37 shows that other disperion-corrected methods are equally valid and so is PBE, which is perhaps not surprising since uncorrected B86bPBE correctly predict 4 out of 7 crystals in this work. Neumann et al.'s method also showed excellent performance in the sixth blind test.[16] There are two points of comparison with the values reported by Brandenburg and Grimme,[37] encapsulated in Table 6 of that work. First, the mean absolute error (MAE) for the X23 using B86bPBE-XDM is 3.56 kJ/mol, to be compared to the best-performing method in Ref. 37 (TPSS-D3) with MAE = 4.6 kJ/mol. Second, the B86bPBE-XDM average rank in Table 5 is 1.7 c.f. the lowest rank in Brandenburg and Grimme, 2.7 (PBE-MBD). This latter comparison is perhaps unfair, since the molecular moieties in the sixth blind test are significantly larger than in previous tests. We expect the good performance of B86bPBE-XDM displayed in this and our previous work will ex-

tend to the sixth blind test systems and to CSP in general. We also note that, since all methods considered by Brandenburg and Grimme[37] are based on GGA functionals, the pitfalls and weaknesses demonstrated in this work will apply to them as well.

In summary, we find that B86bPBE-XDM gives a similar performance to the best available energy ranking methods for crystal structure prediction. B86bPBE-XDM can give significant errors in cases where the base density-functional is not sufficiently accurate (such as for the organic salt), but this is also a potential problem for PW91-D or any other dispersion-corrected GGA functional. B86bPBE-XDM also has the added benefit of having no system-specific parameters and should therefore be more generally reliable for exotic interaction motifs (e.g. compound IX with iodine atoms, see Table 5).

6   Conclusions

In this work, we extended our previous investigation[26] on the suitability of the B86bPBE-XDM approach for the energy ranking step of first-principles crystal structure prediction (CSP) to the remaining non-planar molecules in the CCDC blind tests. The seven compounds studied in this article were found to be more challenging for dispersion-corrected DFT-based energy ranking than the previous planar molecules. One difficulty, evidenced by compound X in the third blind test, is caused by the subtle interplay between intermolecular and intramolecular interactions. It is critical to have an accurate base density functional, ideally with some exact-exchange mixing, for intramolecular conformation changes, in addition to an accurate dispersion method for the treatment of the intermolecular interactions. The underlying cause of this difficulty is delocalization error, which has also been identified in our previous paper[26] as the cause behind the misidentification of the lowest energy structure in compound XIX (an organic salt).

This work also confirms the importance of vibrational free-energy corrections in crystal structure prediction. Thermal effects have now been found to affect the relative stability ordering for 2 of the 21 compounds considered to date from the CSP blind tests, or 10% of cases, which is consistent with the ratio given by Nyman and Day.[24] Thermal effects may also affect the relative free-energy ranking for compound XX; however, it was not possible to perform phonon frequency calculations for this crystal at the present level of theory. Development of more efficient methods for accurate prediction of vibrational free-energy corrections is clearly needed.

Overall, B86bPBE-XDM (without thermal corrections) was found to correctly identify the experimental structure as the free-energy minimum for 16 of the 21 compounds considered in the first five blind tests. This 76% success rate is on par with the best CSP methods presently available, notably the one proposed by Neumann et al., but has the added benefit of reduced empiricism, lacking any system-specific parameterization. Thus, we conclude that the B86bPBE-XDM method is quite promising for first-principles CSP. Ongoing work is directed at making this approach more efficient through use of less computationally-demanding methods for geometry optimization, coupled with DFT-XDM energy evaluations.

The advent of dispersion-corrected density-functional theory (DFT) in the field of crystal structure prediction (CSP), pioneered by Neumann and collaborators, has drastically increased the ability of current protocols to accurately predict the crystal energy landscape of a given compound.[14–16,20–23,26] Although there is little doubt that DFT-based methods outperform most of the previously used force fields in CSP, we hope this and our earlier work[26] will serve as a warning against overconfidence. In particular, the blind test compounds for which B86bPBE-XDM fails to identify the experimental structure as the energy minimum are mostly the same when using Neumann's dispersion-corrected PW91 functional. This suggests that the shortcomings of B86bPBE-XDM also affect other dispersion-corrected GGA methods.

Supporting Information Available: Ta-

bles of the relative energies and crystal volumes per molecule computed for each submitted candidate structure. This material is available free of charge via the Internet at http://pubs.acs.org/.

References

(1) Bauer, J. et al. Ritonavir: An Extraordinary Example of Conformational Polymorphism. *Pharm. Res.* **2001**, *18*, 859–866.

(2) Morissette, S. L. et al. High-throughput crystallization: polymorphs, salts, cocrystals and solvates of pharmaceutical solids. **2004**, *56*, 275–300.

(3) Singhai, D.; Curatolo, W. Drug polymorphism and dosage form design: a practical perspective. *Adv. Drug Deliv. Rev.* **2004**, *56*, 335–347.

(4) Pudipeddi, M.; Serajuddin, A. T. M. Trends in solubility of polymorphs. *J. Pharm. Sci.* **2005**, *94*, 929–939.

(5) Blagden, N.; de Matas, M.; Gavan, P. T.; York, P. Crystal engineering of active pharmaceutical ingredients to improve solubility and dissolution rates. *Adv. Drug Deliv. Rev.* **2007**, *59*, 617–630.

(6) Troisi, A.; Orlandi, G. Band structure of the four pentacene polymorphs and effect on the hole mobility at low temperature. *J. Phys. Chem. B* **2005**, *109*, 1849–1856.

(7) Pfattner, R. et al. High-Performance Single Crystal Organic Field-Effect Transistors Based on Two Dithiophene-Tetrathiafulvalene (DT-TTF) Polymorphs. *Adv. Mater.* **2010**, *22*, 4198.

(8) Jurchescu, O. D. et al. Effects of polymorphism on charge transport in organic semiconductors. *Phys. Rev. B* **2009**, *80*, 085201.

(9) Millar, D. I. et al. The crystal structure of -RDXan elusive form of an explosive revealed. *Chem. Commun.* **2009**, 562–564.

(10) Bolton, O.; Matzger, A. J. Improved Stability and Smart-Material Functionality Realized in an Energetic Cocrystal. *Angew. Chem.* **2011**, *50*, 8960–8963.

(11) Lommerse, J. P. M. et al. A test of crystal structure prediction of small organic molecules. *Acta Cryst.* **2000**, *B58*, 647–661.

(12) Motherwell, W. D. S. et al. Crystal structure prediction of small organic molecules: a second blind test. *Acta Cryst.* **2002**, *B58*, 647–661.

(13) Day, G. M. et al. A third blind test of crystal structure prediction. *Acta Cryst.* **2005**, *B61*, 511–527.

(14) Day, G. M. et al. Significant progress in predicting the crystal structures of small organic molecules - a report on the fourth blind test. *Acta Cryst.* **2009**, *B65*, 107–125.

(15) Bardwell, D. A. et al. Towards crystal structure prediction of complex organic compounds – a report on the fifth blind test. *Acta Cryst.* **2011**, *B67*, 535–551.

(16) Reilly, A. M. et al. Report on the sixth blind test of organic crystal structure prediction methods. *Acta Cryst. B* **2016**, *72*, 439–459.

(17) Grimme, S.; Antony, J.; Ehrlich, S.; Krieg, H. A consistent and accurate ab initio parametrization of density functional dispersion correction (DFT-D) for the 94 elements H-Pu. *J. Chem. Phys.* **2010**, *132*, 154104.

(18) Tkatchenko, A.; DiStasio, R. A.; Car, R.; Scheffler, M. Accurate and Efficient Method for Many-Body van der Waals Interactions. *Phys. Rev. Lett.* **2012**, *108*, 236402.

(19) Neumann, M. A.; Perrin, M.-A. Energy ranking of molecular crystals using density functional theory calculations and an empirical van der Waals correction. *J. Phys. Chem. B* **2005**, *109*, 15531–15541.

(20) Neumann, M. A.; Leusen, F. J. J.; Kendrick, J. A Major Advance in Crystal Structure Prediction. *Angew. Chem. Int. Ed.* **2008**, *47*, 2427–2430.

(21) Asmadi, A. et al. Revisitint the Blind Tests in Crystal Structure Prediction: Accurate Energy Ranking of Molecular Crystals. *J. Phys. Chem. B* **2009**, *113*, 16303–16313.

(22) Kendrick, J.; Leusen, F. J. J.; Neumann, M. A.; van de Streek, J. Progress in Crystal Structure Prediction. *Chem. Eur. J.* **2011**, *17*, 10736–10744.

(23) Neumann, M. A.; van de Streek, J.; Fabbiani, F. P. A.; Hidber, P.; Grassmann, O. Combined crystal structure prediction and high-pressure crystallization in rational pharmaceutical polymorph screening. *Nat. Comm.* **2015**, *6*, 7793.

(24) Nyman, J.; Day, G. M. Static and lattice vibrational energy differences between polymorphs. *CrystEngComm* **2015**, *17*, 5154.

(25) Price, S. L. Computed crystal energy landscapes for understanding and predicting organic crystal structures and polymorphism. *Acc. Chem. Res.* **2008**, *42*, 117–126.

(26) Whittleton, S. R.; Otero-de-la-Roza, A.; Johnson, E. R. The exchange-hole dipole dispersion model for accurate energy ranking in molecular crystal structure prediction. *J. Chem. Theory Comput.* **2017**, *13*, 441–450.

(27) Becke, A. On the large-gradient behavior of the density functional exchange energy. *J. Chem. Phys.* **1986**, *85*, 7184.

(28) Perdew, J. P.; Burke, K.; Ernzerhof, M. Generalized gradient approximation made simple. *Phys. Rev. Lett.* **1996**, *77*, 3865.

(29) Becke, A. D.; Johnson, E. R. Exchange-hole dipole moment and the dispersion interaction revisited. *J. Chem. Phys.* **2007**, *127*, 154108.

(30) Otero-de-la Roza, A.; Johnson, E. R. Van der Waals Interactions in Solids Using the Exchange-Hole Dipole Moment Model. *J. Chem. Phys.* **2012**, *136*, 174109.

(31) Otero-de-la Roza, A.; Johnson, E. R. A benchmark for non-covalent interactions in solids. *J. Chem. Phys.* **2012**, *137*, 054103.

(32) Zhang, Y. K.; Yang, W. T. A challenge for density functionals: Self-interaction error increases for systems with a noninteger number of electrons. *J. Chem. Phys.* **1998**, *109*, 2604–2608.

(33) Ruzsinszky, A.; Perdew, J. P.; Csonka, G. I.; Vydrov, O. A.; Scuseria, G. E. Spurious fractional charge on dissociated atoms: Pervasive and resilient self-interaction error of common density functionals. *J. Chem. Phys.* **2006**, *125*, 194112.

(34) Cohen, A. J.; Mori-Sánchez, P.; Yang, W. Insights into Current Limitations of Density Functional Theory. *Science* **2008**, *321*, 792.

(35) Kim, M.-C.; Sim, E.; Burke, K. Understanding and reducing errors in density functional calculations. *Phys. Rev. Lett.* **2013**, *111*, 073003.

(36) Johnson, E. R.; Otero-de-la Roza, A.; Dale, S. G. Extreme density-driven delocalization error for a model solvated-electron system. *J. Chem. Phys.* **2013**, *139*, 184116.

(37) Brandenburg, J. G.; Grimme, S. Organic crystal polymorphism: a benchmark for dispersion corrected mean field electronic structure methods. *Acta Cryst. B* **2016**, *72*, 502–513.

(38) Giannozzi, P. et al. QUANTUM ESPRESSO: a modular and open-source software project for quantum simulations of materials. *J. Phys.: Condens. Matter* **2009**, *21*, 395502.

(39) Blöchl, P. E. Projector augmented-wave method. *Phys. Rev. B* **1994**, *50*, 17953.

(40) Christian, M. S.; Otero-de-la-Roza, A.; Johnson, E. R. Surface Adsorption from the Exchange-Hole Dipole Moment Dispersion Model. *J. Chem. Theory Comput.* **2016**, *12*, 3305–3315.

(41) Christian, M. S.; Otero-de-la-Roza, A.; Johnson, E. R. Adsorption of graphene to nickel (111) using the exchange-hole dipole moment model. *Carbon* **2017**, (accepted).

(42) Johnson, E. R.; Otero-de-la-Roza, A. Adsorption of organic molecules on kaolinite from the exchange-hole dipole moment dispersion model. *J. Chem. Theory Comput.* **2012**, *8*, 5124–5131.

(43) Togo, A.; Tanaka, I. First principles phonon calculations in materials science. *Scr. Mater.* **2015**, *108*, 1–5.

(44) Hulme, A. T. et al. Search for a Predicted Hydrogen Bonding Motif- A Multidisciplinary Investigation into the Polymorphism of 3-Azabicyclo [3.3.1] nonane-2, 4-dione. *J. Am. Chem. Soc.* **2007**, *129*, 3649–3657.

(45) Price, S. L. From crystal structure prediction to polymorph prediction: interpreting the crystal energy landscape. *Phys. Chem. Chem. Phys.* **2008**, *10*, 1996–2009.

(46) Jetti, R. K. et al. Searching for a polymorph: second crystal form of 6-amino-2-phenylsulfonylimino-1, 2-dihydropyridine. *Angew. Chem. Intl. Ed.* **2003**, *42*, 1963–1967.

(47) Roy, S.; Matzger, A. J. Unmasking a Third Polymorph of a Benchmark Crystal-Structure-Prediction Compound. *Angew. Chem. Intl. Ed.* **2009**, *48*, 8505–8508.

(48) Chan, H.; Kendrick, J.; Leusen, F. J. Molecule VI, a Benchmark Crystal-Structure-Prediction Sulfonimide: Are Its Polymorphs Predictable? *Angew. Chem. Intl. Ed.* **2011**, *50*, 2979–2981.

(49) Neumann, M. A. Tailor-Made Force Fields for Crystal-Structure Prediction. *J. Phys. Chem. B* **2008**, *112*, 9810–9829.

(50) Wu, Q.; Yang, W. Empirical correction to density functional theory for van der Waals interactions. *J. Chem. Phys.* **2002**, *116*, 515.

(51) Wang, Y.; Perdew, J. P. Correlation hole of the spin-polarized electron gas, with exact small-wave-vector and high-density scaling. *Phys. Rev. B* **1991**, *44*, 13298.

(52) Perdew, J. P. et al. Atoms, molecules, solids, and surfaces: Applications of the generalized gradient approximation for exchange and correlation. *Phys. Rev. B* **1992**, *46*, 6671–6687.

(53) LeBlanc, L. M.; Otero-de-la-Roza, A.; Johnson, E. R. Evaluation of shear-slip transitions in crystalline aspirin by density-functional theory. *Cryst. Growth Des.* **2016**, *16*, 6867–6873.

(54) Fronczek, F. R.; Garcia, J. G. (7-endo-Bromocamphorylsulfonyl)imine. *Acta Cryst. E* **2001**, *57*, o996–o887.

(55) Woodcock, H. L.; Schaefer, H. F.; Schreiner, P. R. Problematic energy differences between cumulenes and poly-ynes: Does this point to a systematic improvement of density functional theory? *J. Phys. Chem. A* **2002**, *106*, 11923–11931.

(56) Heaton-Burgess, T.; Yang, W. Structural manifestation of the delocalization error of density functional approximations: C4N+2 rings and C-20 bowl, cage, and ring isomers. *J. Chem. Phys* **2010**, *132*, 234113.

(57) Frisch, M. J. et al. Gaussian 09 Revision A.1. Gaussian Inc. Wallingford CT 2009.

(58) Otero-de-la Roza, A.; Johnson, E. R. Non-Covalent Interactions and Thermochemistry using XDM-Corrected Hybrid and Range-Separated Hybrid Density Functionals. *J. Chem. Phys.* **2013**, *138*, 204109.

(59) Jensen, F. Polarization consistent basis sets: Principles. *J. Chem. Phys.* **2001**, *115*, 9113–9125.

(60) Jensen, F. Polarization consistent basis sets. II. Estimating the Kohn–Sham basis set limit. *J. Chem. Phys.* **2002**, *116*, 7372–7379.

(61) Jensen, F. Polarization consistent basis sets. III. The importance of diffuse functions. *J. Chem. Phys.* **2002**, *117*, 9234–9240.

(62) Johnson, E. R.; Otero-de-la-Roza, A.; Dale, S. G.; DiLabio, G. A. Efficient basis sets for non-covalent interactions in density-functional theory. *J. Chem. Phys.* **2013**, *139*, 214109.

(63) Adamo, C.; Barone, V. Toward reliable density functional methods without adjustable parameters: The PBE0 model. *J. Chem. Phys.* **1999**, *110*, 6158–6170.

(64) Vydrov, O. A.; Scuseria, G. E. Assessment of a long-range corrected hybrid functional. *J. Chem. Phys.* **2006**, *125*, 234109.

(65) Vydrov, O. A.; Heyd, J.; Krukau, A. V.; Scuseria, G. E. Importance of short-range versus long-range Hartree-Fock exchange for the performance of hybrid density functionals. *J. Chem. Phys.* **2006**, *125*, 074106.

(66) Parrish, R. M. et al. Psi4 1.1: An Open-Source Electronic Structure Program Emphasizing Automation, Advanced Libraries, and Interoperability. *J. Chem. Theory Comput.* **2017**,

(67) Otero-de-la Roza, A.; DiLabio, G. A.; Johnson, E. R. Exchange-correlation effects for non-covalent interactions in density-functional theory. *J. Chem. Theory. Comput.* **2016**, ASAP article, DOI: 10.1021/acs.jctc.6b00298.

(68) de Gelder, R.; Wehrens, R.; Hageman, J. A. A generalized expression for the similarity of spectra: application to powder diffraction pattern classification. *J. Comput. Chem.* **2001**, *22*, 273–289.

(69) Otero-de-la Roza, A.; Johnson, E. R.; Luaña, V. Critic2: a program for real-space analysis of quantum chemical interactions in solids. *Comput. Phys. Commun.* **2014**, *185*, 1007–1018.

(70) Macrae, C. F. et al. Mercury CSD 2.0– new features for the visualization and investigation of crystal structures. *J. Appl. Cryst.* **2008**, *41*, 466–470.

(71) Heit, Y. N.; Beran, G. How important is thermal expansion for predicting molecular crystal structures and thermochemistry at finite temperatures? *Acta Cryst. B* **2016**, *72*, 514–529.

(72) Johnson, E. R.; DiLabio, G. A. Structure and binding energies in van der Waals dimers: Comparison between density functional theory and correlated ab initio methods. *Chemical physics letters* **2006**, *419*, 333–339.

Graphical TOC Entry